



Mediterranean aegagropiles from *Posidonia oceanica* (L.) Delile (1813): a first complete description from macroscopic to microscopic structure

Laurence Lefebvre¹ · Philippe Compère² · Angélique Léonard³ · Erwan Plougonven³ · Nicolas Vandewalle⁴ · Sylvie Gobert^{1,5}

Received: 19 May 2020 / Accepted: 15 January 2021

© The Author(s), under exclusive licence to Springer-Verlag GmbH, DE part of Springer Nature 2021

Abstract

Aegagropiles are round-shaped conglomerations of *Posidonia oceanica* debris commonly found along the coasts of the Mediterranean Sea. This study presents a detailed description of the composition of aegagropiles in terms of their internal organisation in different layers (and the orientation of the fibres in these layers), the proportion of constituent elements (fibres and minerals) and the histological (by way of microscopic observations) nature of all of these aegagropiles elements. The aim of this work is to take a detailed interest in the structure of the aegagropiles of *Posidonia oceanica* and to determine the process that forms them. Aegagropiles are an assemblage of two types of debris from the *P. oceanica* meadow: (1) plant-based: fibres more or less degraded from *P. oceanica* shoots (leaves and rhizomes) and (2) mineral particles such as silicates and biotic Ca-carbonate debris. On the basis of structural and compositional observations, we proposed an elucidation of the cycle in several phases: initiation of a “roll” by aggregation of litter fibres and sand in the ripple marks, growth, breakdown of the roll into small balls (microbial and mechanical degradation) and export of aegagropiles down (into the abyss) or on to the beaches. Calculations estimate that considering its density of 0.2 g/cm³, an aegagropile represents the accumulation of fibres from approximately 25 shoots of *P. oceanica*.

Introduction

Along the beaches of the Mediterranean Sea, egg-shaped conglomerations of plant debris, named “aegagropiles”, are commonly found, varying in size from millimetres to centimetres (Verhille and Le Gal 2012, 2013). These phenomena can cover large areas, especially after storms. Research shows that aegagropiles are formed by hydrodynamic movements and are made of different plant fibrous elements (*Posidonia oceanica*) and sand grains (Ganong 1905; Mathieson et al. 2015, 2016). These hydrodynamic movements in sand ridges, called ripple marks, cause the litter from marine meadows to accumulate. After an unknown amount of time, this litter forms aegagropiles (Mackay 1906; Boudouresque et al. 2006; Verhille and Le Gal 2012, 2013).

An accumulation of dead leaves, rhizomes and roots of *P. oceanica* is common along the Mediterranean coast forming imposing masses on the beaches. The clusters, called “banquettes”, comprising a thickness of a few centimetres to several metres, can reduce the beach erosion rate (Boudouresque and Meinesz 1982; Boudouresque et al. 2006; Gobert et al. 2006; Vacchi et al. 2012). Aegagropiles are also found on these beaches, carried in on the waves. The banquettes

Responsible Editor: C. Wild.

Reviewers: Undisclosed experts.

✉ Laurence Lefebvre
l.lefebvre@uliege.be

¹ Laboratory of Oceanology, MARE Centre, FOCUS, University of Liège, Allée du 6 Août, 15, Sart Tilman, B6c, 4000 Liège, Belgium

² Laboratory of Functional Morphology and Evolution, UR-FOCUS, MARE Centre and Centre for Applied Research and Education in Microscopy (CAREM), University of Liège, Sart Tilman, B6c, 4000 Liège, Belgium

³ Chemical Engineering–Products, Environment and Processes (PEPs), University of Liège, Sart Tilman, B5, 4000 Liège, Belgium

⁴ GRASP, CESAM Research Unit, University of Liège, Sart Tilman, B5a, 4000 Liège, Belgium

⁵ STARESO, Pointe Revellata, BP33, 20260 Corse, France

and the aegagropiles are often found in larger quantities after storm events. On occasion, aegagropiles somewhat smaller in size than average may be found within the banquettes (Lefebvre observation).

Several similar formations of plant or algal debris have been described along beaches or rivers, i.e. conglomerations of other seagrasses such as *Zostera nodosa* (Ucria 1793) (Kuo and Stewart, 1995) or *Ruppia maritima* (L., 1753) (Olson et al. 2005), as well as some green algae (Chlorophyta) such as the *Cladophora* genus (Kütz, 1843) (Schreb., 1789; Acton 1916) or *Chaetomorpha picquotiana* (Mountain ex Kütz, 1849) (Mathieson and Dawes 2002). According to Austin and Wilce (1960), this type of conglomerate is formed by red algae (Rhodophyta) *Furcellaria lumbricalis* ((Hudson) Lamouroux, 1813) (Austin, 1960) and brown algae (Phaeophyta) *Phylaiella littoralis* ((Linnaeus) Kjellman 1872) (Wilce et al. 1982).

In *Posidonia oceanica* (L.) Delile, the annual cycle of sexual reproduction begins with autumnal hydrophilic pollination. Six to nine months later (May–July), the plant releases mature fruits. After floating for several weeks, the pericarp rots, leaving the seed to sink to the ocean floor. If the substrate and conditions are favourable, the seed develops roots and produces a new plant. Asexual reproduction also occurs by extension of the stems (orthotropic

and plagiotropic) (Giraud 1977; Boudouresque and Meinesz 1982; Smith and Walker, 2002; Boudouresque et al. 2006; Gobert et al. 2006). The leaves of the plant fall within 5–8 months (rarely lasting up to 14 months), falling at a higher rate in autumn due to lower light and stormy weather (Fig. 1 II). The scission that allows the leaves to fall takes place at the ligula (between the leaf blade and the petiole), while the petiole (also called the leaf sheath) remains on the rhizome. The accumulation of *P. oceanica* leaves on the seabed (Fig. 1 II, IV), along with other plant debris (algae, rhizomes, roots) mixed with epiphytes, constitutes the litter under consideration (Fig. 1 III) (Boudouresque and Meinesz 1982; Pergent 1990; Gobert et al. 2002; Gobert et al. 2006; Boudouresque et al. 2006). This litter will either form sediment on the seabed (from beaches (Fig. 1 I) to abyss (Fig. 1 IV)) or be degraded by macro- and microorganisms and abiotic factors (Pergent et al. 1994). On beaches, the accumulation of this debris forms a structure called a “banquette” (Fig. 1 I), from a few centimetres to several metres thick. These formations can reduce the rate of erosion (Boudouresque and Meinesz, 1982; Boudouresque et al. 2006; Gobert et al. 2006; Vacchi et al. 2012). The seagrasses constitute an annual net production of 0.6×10^9 tonnes of carbon per year (1.13% of total marine primary production) (Duarte and Cebrian 1996; Duarte and Chiscano 1999) and represent a

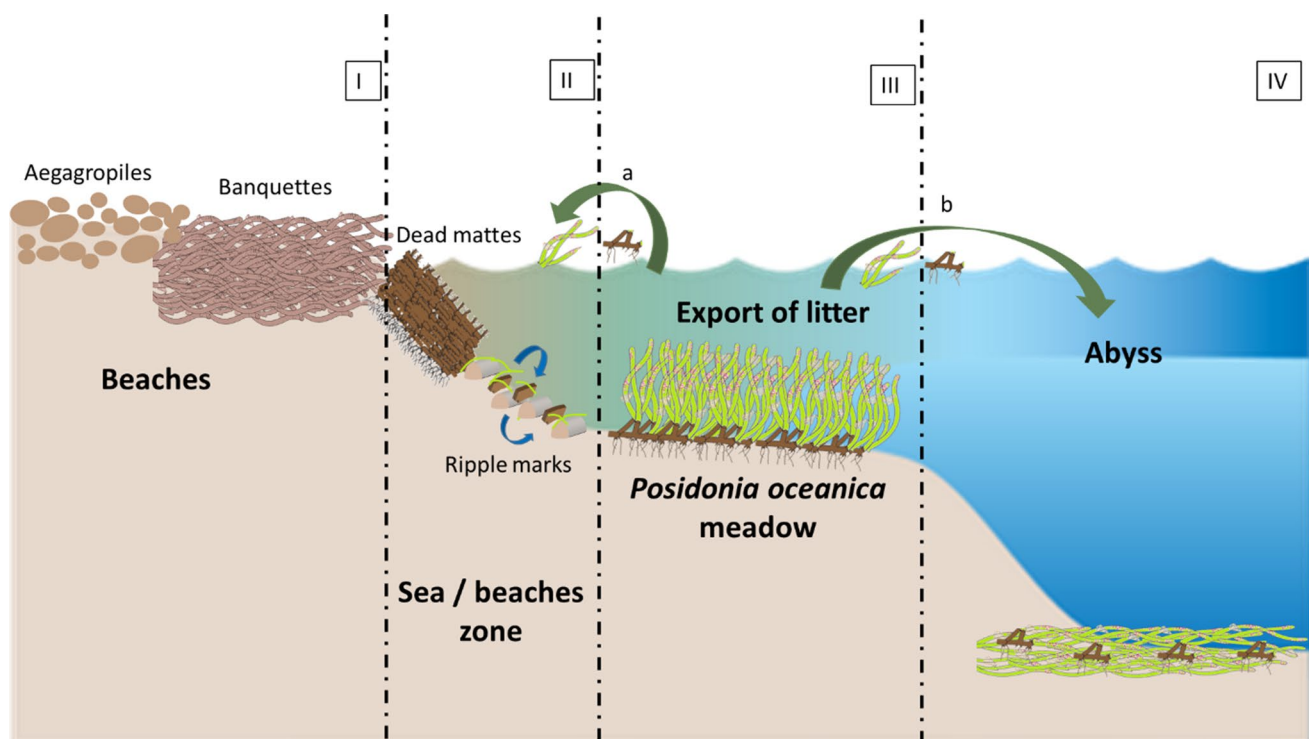


Fig. 1 The export of *Posidonia oceanica* organs from the meadow. I: beaches with aegagropiles and banquettes II: the sea/beach zone with dead mattes and meadow organs a in ripple marks with the hydro-

dynamics at shallow depth III: *Posidonia oceanica* meadow with its coastline export a and b to the abyss IV: the abyss with the clusters of the various organs of the meadow

submarine carbon sink of 0.08×10^9 tonnes of carbon per year worldwide (Hemminga and Duarte, 2000). This carbon sink is due to the low turnover of the organic matter constituting the meadow and its storage in the mattes and the litter (Hemminga and Duarte 2000; Gobert et al. 2002; Larkum et al. 2007; Ababie et al. 2016). Marine magnoliophyte formations are thought to be responsible for 40% of the carbon fixed each year by coastal vegetation, with variations depending on the species and environmental conditions (Laffoley and Grimsditch 2009). In the Mediterranean Sea, mattes capture 4 to 5 times more carbon than other meadow species (Larkum 1989; Duarte and Cebrian 1996; Hemminga and Duarte, 2000; Gobert et al. 2002; Duarte et al. 2005; Larkum et al. 2007; Gobert et al. 2006).

There are no studies focussed on the origin, structure and composition of *Posidonia oceanica* aegagropiles (Cannon 1979; Vizzini et al. 2003; Verhille and Le Gal 2012, 2013; Coletti et al. 2013). The present study deals with these aspects. The structure of the aegagropiles of *P. oceanica* was meticulously investigated from the macroscopic level (shape, size, internal layers, density) to the microscopic levels by characterising their components and mechanical and microbial alterations. The collected data detail the origin of the components and shed light on the lifecycle of this phenomenon (formation, evolution and final degradation).

Materials and methods

Biological material and measurements

One hundred and fifty-nine *P. oceanica* aegagropiles were collected along the beach of Calvi (Corsica, France) (42° 35' 04" N; 008° 43' 39" E) in April 2016. The sampling was conducted prior to the cleaning of the beaches carried out each season before the beginning of the tourist season.

Preparation of entire aegagropile

Freeze-fractures

For observation of their internal organisation, six aegagropiles were frozen in liquid nitrogen and cut into 5 mm broad slices using a metal knife. The slices were first observed with a stereomicroscope (CETI Steddy) and then photographed.

Four of the freeze-fractures were then glued onto glass slides with double-sided carbon tape and surrounded with silver paint to create an electric contact up to their upper side before being Pt-coated in a sputter-coater (Balzers SCD-030, Liechtenstein) and viewed in SEM in a high-vacuum condition.

Polished slices

Fourteen aegagropiles of different sizes and shapes were selected for making polished slices according to the three following orientations: frontal, sagittal and at least at two transversal levels. In order to remove the residual concentration of water 10–20%, the fourteen aegagropiles were placed in a bath of 100% ethanol for 24 h at 4 °C. Seven of these were contrasted by immersion for 5 days in a 0.25% gadolinium acetate solution in 100% ethanol at 4 °C (Hosogi et al. 2015). These seven aegagropiles were rinsed in a solution of 50% ethanol with 50% of the contrasted solution at room temperature for 2 days, then twice in a bath with 50% ethanol at room temperature for 1 h, followed by 5 days in 100% ethanol with 3 renewals at room temperature. All samples were dehydrated in two baths (24 h) in absolute ethanol, followed by 3 baths (24 h) in pure acetone at room temperature. They were then embedded in epoxy resin (Epofix Kit, Struers, with 1/30 initiator). For resin impregnation, the samples were immersed in a 1: 1 acetone-resin mixture (48 h) under a hood. For resin embedding, the complete aegagropiles were placed and maintained in a Tetra-pack vessel filled with pure Epofix resin. In order to evaporate acetone and residual gas bubbles (from the plant cell lumens), the samples were pumped in a vacuum oven (Heraeus) under 100 mbar (12 h), then placed under a hood (48 h) and left to polymerise for 14 days at 60 °C. The resin-embedded aegagropiles were sliced with a hacksaw to isolate 2.5–3 mm thick sections. The thick sections were then glued with Epofix resin on geological glass slides and left to polymerise (for 24 h) at 60 °C. The thick sections were progressively thinned by polishing under a flow of water in a Rotapol-2 (Struers) polishing machine using silicon carbide sandpapers with increasing grit size (80, 220, 800, 1200, 4000 grain/inches²). Final mirror polishing was done with a diamond suspension (3 µm, 1 µm) on a velvet disc (Kuo and den Hartog 2007; Lepot et al. 2014).

To highlight the *P. oceanica* debris (fibres) and facilitate their identification and orientation in light microscopy (LM), the polished slices (not previously contrasted in gadolinium acetate) were stained with toluidine blue (1%, pH 9.0) as is typically done with semi-thin sections of resin-embedded tissues (Hayat 1993; Kuo and den Hartog 2007; Lepot et al. 2014; Hosogi et al. 2015). The plant debris was identified and counted on seven aegagropiles, and the orientation of the fibres was determined according to the section plane. In order to characterise the density and arrangement of the debris, 267 images were taken along the large (*D*) and small (*d*) diameters of the aegagropile sections for the 3 defined zones (see results): peripheral (L 1), median (L 2 + L 3) and central (nucleus). The density of the plant debris and minerals in the aegagropiles was measured. The plant debris was classified in 4 categories with 2 relating to the shape of their

transversal section (circular or flattened) and 2 reflecting the orientations of their section according to the polished surface: longitudinal (noted as CL) or transverse (noted as CT). In addition, the origin (leaves, roots, basal sheath of leaves or stem) of each part of the plant debris was determined.

Isolated fibres

In this study, we chose to name all the plant components “fibres” without regard to their origin (*Posidonia oceanica* or algae) or their histological nature (leaves, roots, parenchyma, epidermis, etc.).

Fibre selection

Isolated fibres were collected from four transversal freeze-fractures: two from each type of aegagropile, comprising homogeneous ball-shaped and heterogeneous egg-shaped (Fig. 2).

The sampling was carried out by taking 20 fibres using forceps at 3 different places within each layer (see result part). This represents 60 fibres per layer, in four layers per aegagropile and in four aegagropiles, totalling 960 fibres. Each fibre was photographed and measured (length and width), and 3 morphotypes were identified.

All aegagropiles were measured and weighed after drying (48 h) to obtain their density.

Fibre characterisation

For surface characterisation, 15 fibres of each shape (thin, flat and wide) from the four aegagropiles were glued onto glass slides with double-sided carbon tape, Pt-coated (Balzers SCD 030 sputtering unit) before SEM observation.

For histological observation, another set of 15 isolated fibres was fixed by immersion for 1 h in 2.5% glutaraldehyde in Na-cacodylate 0.1 M at pH 7.4, briefly rinsed in double-distilled water, then post-fixed for 1 h in 1% OsO₄ at 20 °C, and rinsed thrice for 10 min in double-distilled water. Samples were dehydrated through an ethanol series up to 100% ethanol (3 × 20 min) and 1.2 propylene oxide. They were impregnated for 2 h 30 in 1:1 resin Epon 812 (SPI-Pon 812 Embedding kit, SPI Supplies, USA)-1.2 propylene oxide mixture. The evaporation/polymerisation procedure was the same as previously described for whole aegagropiles. Transversal semi-thin sections were cut at 1 µm using a glass knife on an ultra-microtome (Porter-Blum MT2) and stained with toluidine blue (1%, pH 9.0) to be observed with light microscopy (Hayat 1993; Kuo and den Hartog 2007).

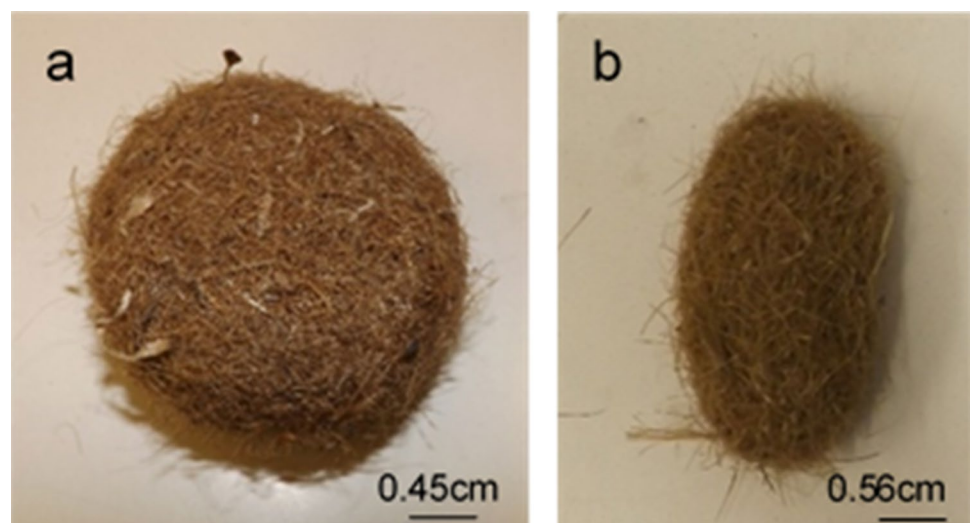
Observation techniques

Macroscopic observations and pictures of freeze-fractured aegagropiles ($n = 6$) and isolated fibres ($n = 960$) were made with a stereomicroscope (CETI Steddy) fitted with a VisiCam 5.0 camera and image capture software.

X-ray micro-computed tomography (µCT) scans were made on six aegagropiles with a Bruker Skyscan 1172G. The X-ray source voltage was set at 50 kV, and the images were taken with a pixel size of 13.64 µm with 2 by 2 binning, 480 ms exposure time per projection, and a rotation step of 0.2° over 360°. The tomographic reconstructions were computed with the NRecon software, v.1.6.10.1 (Holdsworth and Thornton 2002).

Light microscopy observations and images were made on 2 different types of equipment: an Olympus PROVIS AX70 equipped with a VisiCam 5.0 camera (VWR) and software for image capture for semi-thin sections of 15 fibres per type (see above) and an Olympus CX21 with a Motic camera and

Fig. 2 Shapes of *P. oceanica* aegagropiles **a** Spheroidal or ball-shaped. **b** Ellipsoidal or egg-shaped



Motic Images 3.0 software for the thin polished slices (in the three planes of space, i.e. frontal, sagittal and at least at two transversal levels on fourteen aegagropiles) image capture (see above).

SEM-imaging was carried out on an ESEM-FEG XL-30 (FEI/Philips, Netherlands) and an ESEM Quanta 600 (FEI/Philips, Netherlands). Bulk specimens, i.e. fractured aegagropiles and isolated fibres (15 fibres/morphotype), were visualised in high vacuum (10^{-7} Torr) with an E-T secondary electron detector (SE-SEM) at 20 kV accelerating voltage (see above). Polished slices Gd—contrast and noncontrast samples ($n=14$) were visualised at low vacuum (0.4 Torr) with a backscattered electron detector (BSE-SEM) and 20 kV accelerating voltage (see above). In order to reinforce the contrast of organic fibres, some of the polished slices were contrasted for 10 min in alcoholic uranyl acetate—(UO)Ac—according to the classical staining method for electron microscopy (Kuo and den Hartog 2007).

The elemental X-ray microanalyses were made in the ESEM—FEG XL-30 (FEI/Philips, Netherlands) equipped with a silicon drift detector (SDD Bruker, 129 eV and 10 mm², Nano GmbH Inc., Germany) with a Super Ultra-Thin Window (S-UTW) for the detection of lighter elements down to boron. The X-ray signals were analysed using the Quantax ESPRIT 2.1 software (Bruker, Germany) to produce elemental spectra, semi-quantitative data (standardless ZAF correction) and elemental distribution maps. These microanalyses were carried out on the thin polished slices (see above).

Statistical analysis

Statistical analysis of the internal structure was performed on data collected from the thin polished slices and the measurement of fibre width. Statistical analysis was performed with the R* software v.3.3.1. (RStudio Team, 2015). For statistical tests, the Kruskal–Wallis and the Wilcoxon–Mann–Whitney tests were used. For graphical representations, boxplots, histograms and principal component analysis (PCA) were used.

Results

External morphology

Among the one hundred and fifty-nine aegagropiles of our sampling, 21% were spherical (ball-shaped), and the others displayed rather an ellipsoidal shape (egg-shaped). In the egg-shaped aegagropiles, large woody debris sometimes emerged from the ellipsoidal ends. The density of aegagropiles varied between 0.10 and 0.40 g/cm³ with an average of 0.22 ± 0.04 g/cm³ (Fig. 3).

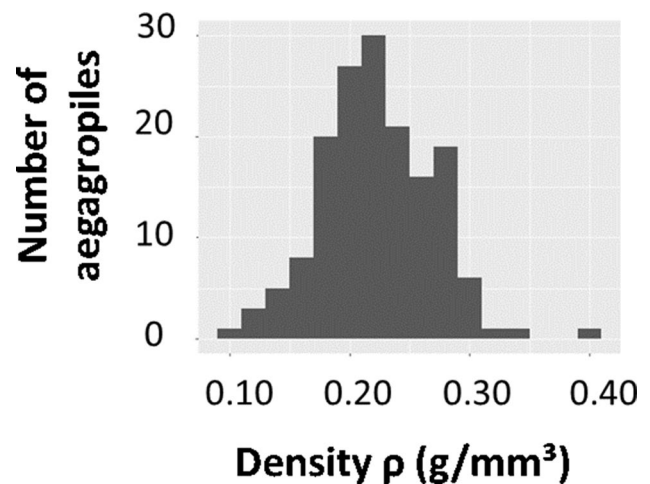


Fig. 3 Density distribution of Calvi aegagropiles

Internal morphology

Internal architecture

Based on macroscopic observations of freeze-fractures (Fig. 4) and polished slices, and in agreement with X-ray projections (Fig. 5), three types of aegagropiles were distinguished: heterogeneous and homogeneous, i.e. with or without a distinct nucleus, and an intermediate type. The first two types of aegagropiles roughly corresponded to ellipsoidal and spheroidal shapes, respectively. In 58% of cases, the ellipsoidal aegagropiles were correlated with the heterogeneous type or the rhizomic nucleus. In addition, all of them exhibited successive concentric layers (Fig. 4) of varying texture, with changes in composition in plant fibres and mineral sandy grains as well as thickness. In the heterogeneous aegagropiles, the central nucleus was white-coloured and often contained a recognisable piece of rhizome that sometimes emerged at the end(s) of the long axis. In the intermediate aegagropiles, the rhizomic piece in the nucleus was replaced by several clusters of dark pieces or fibres. In contrast, the homogeneous aegagropiles had an indistinct nucleus (Fig. 5).

The concentric fibrous layers were the same in both types of aegagropiles: from the outer surface to the centre, the layers were labelled as follows: superficial layer (L 1), median layer (L 2) and deep layer (L 3) surrounding the nucleus (L 4 or Nu). Macroscopically, the superficial layer (L 1) comprised scarcely distributed fibres, while the median layer appeared relatively fibre-rich, and the deep layer was distinguished by a higher proportion of sandy particles together with fibres, giving a whitish colour and a more compact aspect. However, on the polished slices,

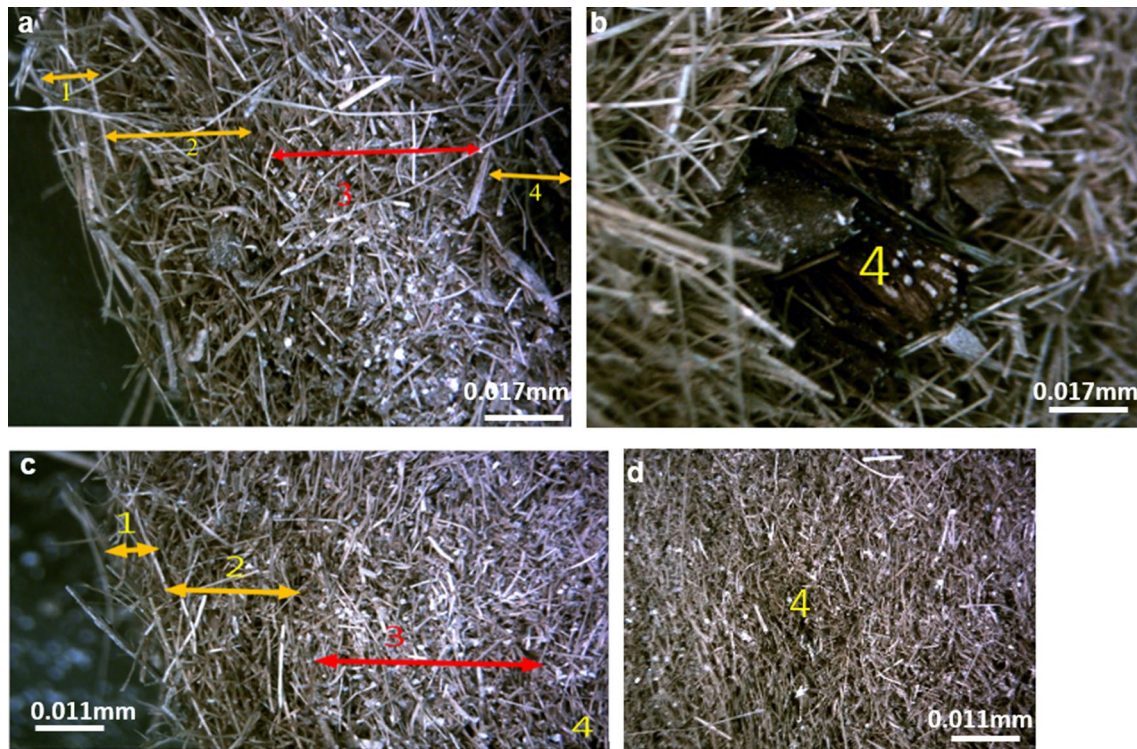


Fig. 4 Stereo-microscope photographs illustrating the two types of aegagropiles. **a** Heterogeneous aegagropile with the 3 layers (1, 2 and 3) and the nucleus (4), **b** magnification of the nucleus (4), **c** homoge-

neous aegagropiles with the 3 layers (1, 2 and 3) and the nucleus (4), **d** magnification of the nucleus

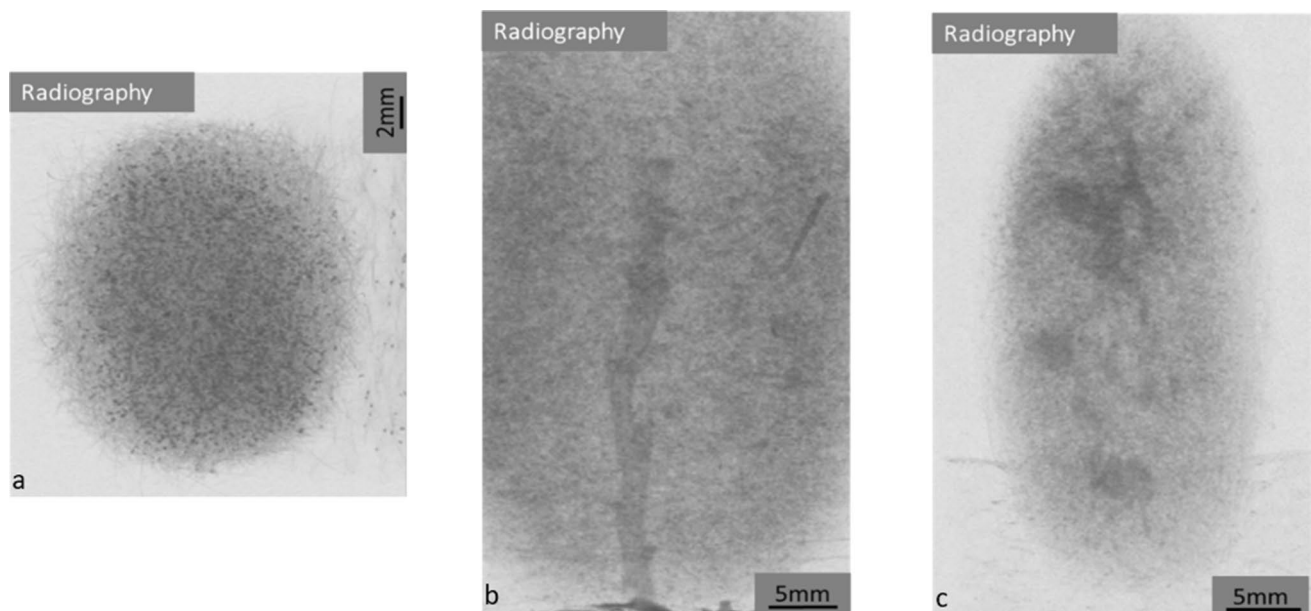


Figure 5 X-ray projections from the μ CT scans of three different aegagropiles. **a** Homogeneous (ball-shaped) type with indistinct nucleus **b** Heterogeneous (egg-shaped) type with a unique (woody or rhizomic) nucleus **c** Intermediate type with several degraded rhizomic fragments

the L 2 and L 3 layers were difficult to distinguish, and the nucleus of homogeneous aegagropiles did not appear very different from layer L 3.

Characterisation of the layers

Relative thickness of the layers

Measurements made on six freeze-fractured samples showed that the three layers and the nucleus maintained roughly similar thicknesses regardless of the aegagropile type. The superficial layer was always the thinnest (2.35 ± 0.41 mm of L 1, representing 14% of the entire aegagropile), while the deep layer (L 3) had the highest thickness (7.95 ± 1.88 mm, reaching 44% of the entire aegagropile). The nucleus itself (3.27 ± 1.35 mm) represented 17% of the entire aegagropile (Table 1).

Fibre density and distribution of fibre categories

The morphometric analysis of the fibres in the 3 concentric layers and the nucleus revealed that the layers differed in

fibre density and mineral particles, and in the types of fibres as defined in Table 2.

Counting fibre sections and mineral particles on the polished slices (homogeneous or heterogeneous type) (Table 3 and Fig. 6) confirmed that the superficial zone (L 1) presented fewer fibres ($12 \pm 2\%$ section surface of fibres/unit of section surface) and mineral particles ($1.2 \pm 0.9\%$ section surface of mineral/unit of section surface) than the internal zones. Fibre density increased significantly in the median zone (L 2 + L 3) ($18 \pm 4\%$ section surface of fibres/unit of section surface). The density of mineral particles also increased ($7 \pm 2\%$ section surface of minerals/unit of section surface), appearing to constitute a type of cement around the central zone. The central zone was different for the homogeneous and heterogeneous types. In the latter, this zone corresponded to the nucleus, where a higher fibre density ($26 \pm 4\%$) resulted from having larger fibres or a woody piece found together with minerals ($1.0 \pm 0.9\%$). In the former, the density of fibres and mineral particles did not differ from those in the L 3 ($19 \pm 5\%$ of fibre section surface and $3 \pm 2\%$ mineral section surface).

Table 1 Diameters (mm) and proportional thickness (in %) of the different layers in the two types of aegagropiles (mean value \pm SD)

Aegagropile type	Aegagropile diameters (mm)	Thickness of layer 1 (%)	Thickness of layer 2 (%)	Thickness of layer 3 (%)	Thickness of nucleus (%)
Heterogeneous aegagropiles	36.15 ± 0.16	12.5 ± 0.7	24 ± 4	46 ± 8	17 ± 4
Homogeneous aegagropiles	42.66 ± 5.74	14 ± 3	26 ± 3	43 ± 4	17 ± 3

Table 2 Width, flexibility and external aspect of three morphotypes of fibres composing the *P. oceanica* aegagropiles




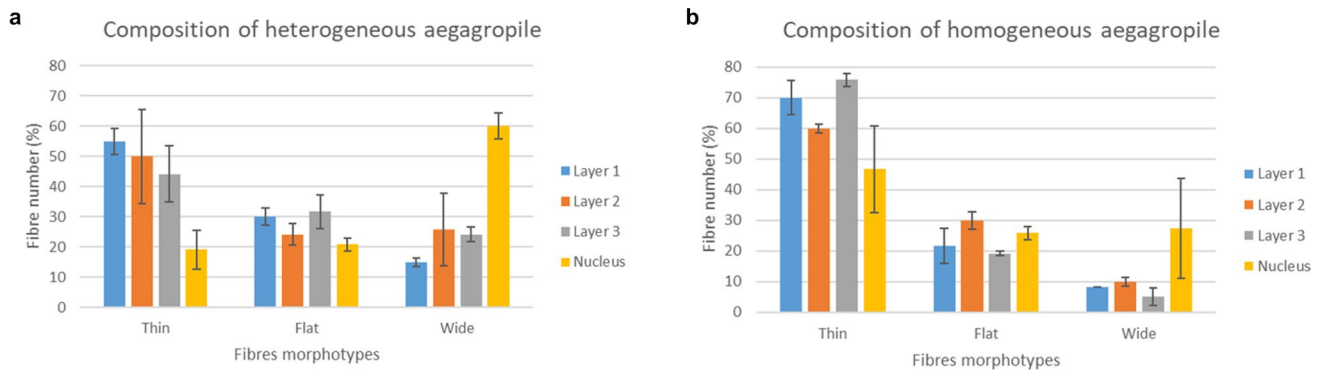
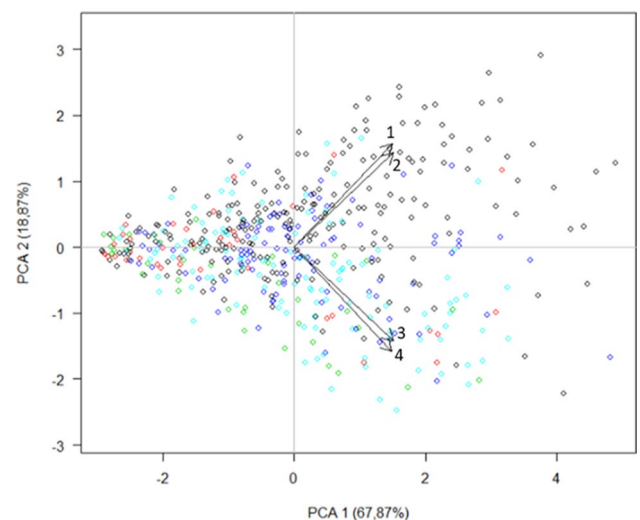
Type of fibre	Width (\pm SD)	External appearance	Picture
Thin	0.142 ± 0.051 mm	Flexible +++	
Flat	0.462 ± 0.095 mm	Flexible ++	
Wide	2.295 ± 1.380 mm	Flexible +	

Table 3 Distribution of mineral particles and fibres (%) in the layers of the two types of aegagropiles

Aegagropile type	Localisation (name of zone)	Mean values % (section surface of fibres/unit of section surface) \pm SD	Mean values % (section surface of minerals/unit of section surface) \pm SD
Homogeneous	Layer 1 (peripheral)	12 \pm 2	1.2 \pm 0.9
	Layer 2 + 3 (median)	18 \pm 4	7 \pm 2
	Nucleus (central)	19 \pm 5	3 \pm 2
Heterogeneous	Layer 1 (peripheral)	12 \pm 2	1.2 \pm 0.9
	Layer 2 + 3 (median)	19 \pm 4	7 \pm 2
	Nucleus (central)	26 \pm 4	1.1 \pm 0.9

**Fig. 6** Histograms representing the proportions of different fibre types (flat, intermediate and wide) in percentages of the total fibre content within the 4 layers (layer 1 in blue, 2 in orange, 3 in grey andnucleus in yellow) of aegagropiles. **a** Heterogeneous aegagropiles and **b** Homogeneous aegagropiles

The measurements of the widths of 960 fibres (Fig. 6) from all 4 layers of the four aegagropiles (2 for each type) showed that the narrow fibres dominated in the superficial layer (70% of thin fibres for the homogeneous type and 55% of thin fibres for the heterogeneous type), while the median layer comprised a mixture of fibres belonging to the three categories with a higher proportion of thin fibres than of the other morphotypes (flat or wide). In homogeneous aegagropiles, the L 2 was made up of 60% thin fibres, 30% flat fibres and 10% wide fibres. In heterogeneous ones, by comparison, the same layer consisted of 50% thin fibres, 24% flat fibres and 26% wide fibres. In contrast, wide fibres appeared more numerous in the deep layer and the nucleus, especially in the heterogeneous aegagropiles. An examination of the fibre composition in the L 3 layer in the homogeneous aegagropiles revealed that 76% were thin fibres, 19% were flat fibres and 5% were wide fibres. In comparison, in the heterogeneous aegagropiles, the proportion of wide fibres reached 24%, while flat fibres represented 32%, and only 44% of the fibres were of the thin type. The proportion of wide fibres was also considerably higher within the nucleus layer. The homogeneous aegagropiles exhibited the following composition: 47% thin fibres, 26% flat fibres and 28% wide fibres. In contrast,

**Fig. 7** Graph combining the PCA (correlation circle) and the distribution of the data in the form of a point cloud according to PC1 and PC2. 1. CT round, 2. CL round, 3. CT long, 4. CL long. The 4 different layers: central zone or nucleus (black), median zone with layers 2 and 3 (red and green) and layer 1 or peripheral zone (blue and sky-blue)

the heterogeneous aegagropiles were made up of 19% thin fibres, 21% flat fibres and 60% wide fibres.

Compilations of architectural results in a principal component analysis (Fig. 7)

In the principal component analysis (PCA) (Fig. 7), the first principal component (PC1) (68%) was negatively correlated with the 4 variables (CTround, CLround, CLlong and CTlong) and was therefore linked to the general fibre density in the different layers. The second principal component (PC2) (19%) differentiated the round sections (CTround, CLround), which were positively correlated, from the long ones (CLlong, CTlong). These two components explain 87% of the variability. In the peripheral zone (blue and sky-blue) and the median zone (L 2 and L 3) (red and green), long sections (CTlong and CLlong) were more abundant (positive in PC1). The central zone (Nucleus) (black) presented more rounded sections (CTround and CLround) and was found in the positive side of PC2. Moreover, the longitudinal fibres (CLround and CLlong) were found mainly in the thin polished sections cut longitudinally, while the transverse fibres (CTround and CTlong) were mainly found in the thin polished sections cut transversely.

Internal components

Fibres

Furthermore, the fibres categorised in three types (Table 2) were also characterised through observation in LM (Fig. 8a–c) and SE-SEM and BSE-SEM (Fig. 8d–h) and compared with fresh organs (roots, leaves, stems) of *P. oceanica* identified on fractures (Fig. 8e, f, g) and polished slices (Fig. 8d). Thin fibres had round-shaped sections (Table 2 and Fig. 8a, d, e) similar to those of *P. oceanica* stems (Fig. 8a, e), with a corresponding diameter ($0.11 \text{ mm} \pm 0.02 \text{ mm}$).

Flat fibres were long, flat fragments a few cells in thickness (Table 2 and Fig. 8b, f), including a layer of thick-walled sclerenchyma cells covered, or not, by the thin-walled epidermal cells (Fig. 8b, f, g). All these fibres were probably fragments of *P. oceanica* sheaths and leaves because flat fibre of the unique sclerenchyma cell layer are characteristic of leaves, were they form small isolated bundles, and of sheaths were they form a continuous layer below the epidermis. Their measured width was $0.19 \pm 0.03 \text{ mm}$. Wide fibres appeared as large irregular but flattened fragments of $0.57 \pm 0.31 \text{ mm}$ of mean width. They included numerous cell columns belonging to several cell types and tissues, including parenchyma cells, complicating their identification (Fig. 8c, d). Indeed, due to the lack of other typical

structures, this type of fibre was presumed to come from *P. oceanica* rhizomes.

On the other hand, the observations gave evidence of differing degrees of alterations to the aegagropiles, especially in the cell walls (Fig. 8h). The wide fibres were slightly altered, having lost at least the outer cell wall of the epidermis (with cuticle), and some epiphytic organisms, such as diatoms, had colonised their surface. Deeper degradations were observed on thin fibres that appeared to delaminate longitudinally in the thinner fibres of a few cell columns (Fig. 8h). This degradation by separation of cell columns seemed to be due to the disappearance of the middle lamella between adjacent cells. This phenomenon created visible spaces between cells, as seen in fractures and semi-thin sections of each kind of fibre (Fig. 8a, c, g, h). Flat fibres also showed some degradation, although less than the thin type (Fig. 8h). The fibres were often covered by epiphytic micro-organisms, such as diatoms and bryozoans. These diatoms were found on the cuticle of the intact epidermis or in empty cells.

Other plant debris and minerals

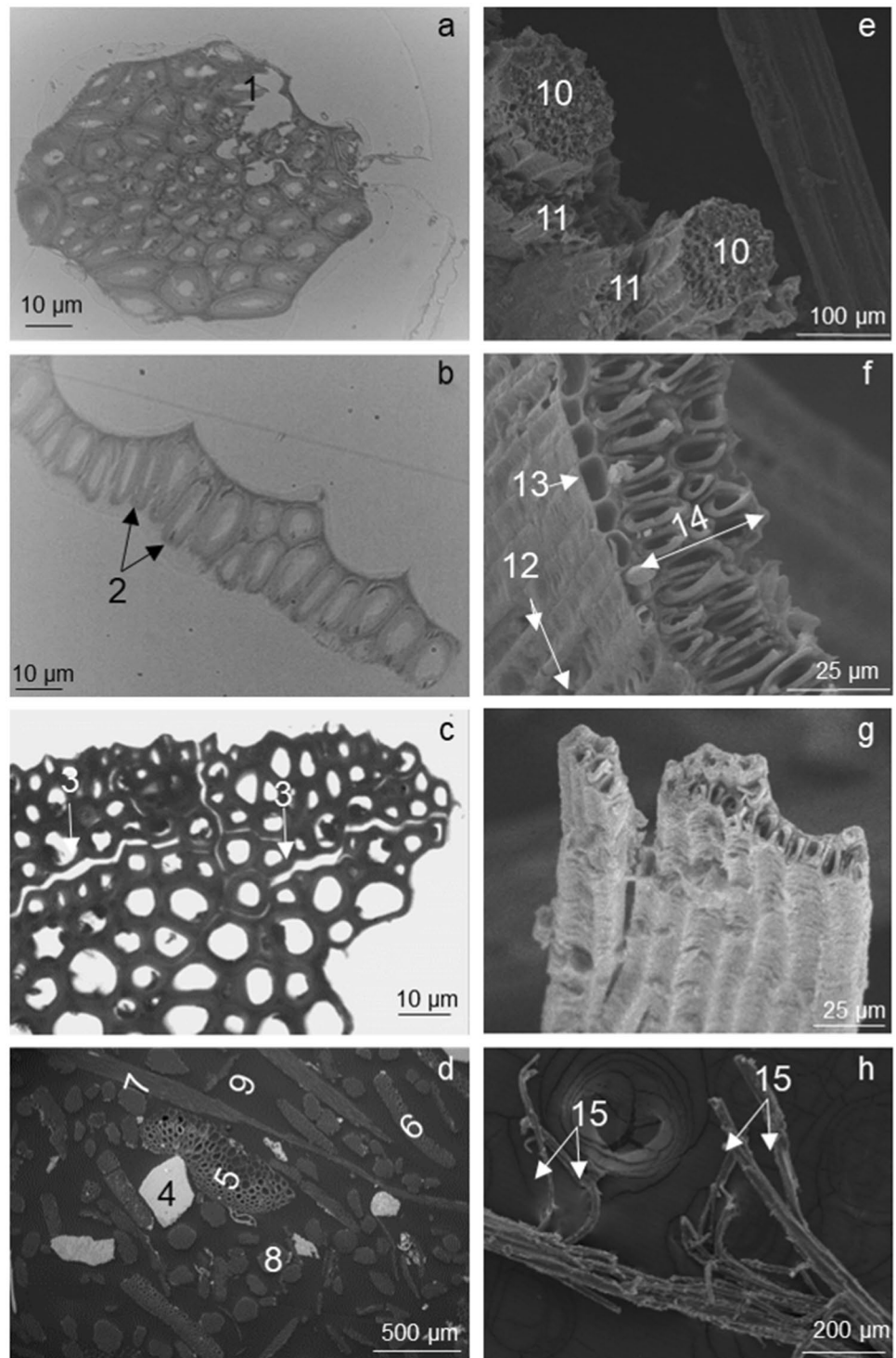
In addition to the fibres, the central or axial layers often contained mineral particles and one or more large “woody” plant remains that were obvious on freeze-fractures and polished slices (Fig. 9). These fragments were most often identified as poorly altered fragments of rhizomes.

The elemental X-ray spectra and mappings obtained by EDAX on the polished slices provided the elemental composition of the plant debris and mineral particles inside the aegagropiles under examination (Fig. 9). The spectra showed that the plant debris typically contained C, O, Si, S, Ca, Fe, while U and Cl came from the contrasting agent (UO) Ac and from the embedding resin, respectively. The elemental mappings showed two distinct kinds of mineral particles: Si-rich and Al-rich particles that likely corresponded to aluminosilicates and Ca-rich particles, probably Ca-carbonate fragments of invertebrate shells, as also suggested by some morphologies (Fig. 9).

Discussion

Categorised as two types, Mediterranean seaballs or aegagropiles exhibit two roughly corresponding internal architectures. The observations confirmed that they mainly comprised *P. oceanica* debris, and most of their fibres were parallel to the surface. Four concentric layers were distinguished on the basis of fibre density and the proportion of each fibre morphotype, as well as fibre and mineral particle density, with the innermost layer occupied either by a large fragment or simply more fibres. The fibres were classified

Fig. 8 Illustrations of the 3 categories of fibres found in *P. oceanica* aegagropiles as viewed on LM-images (**a–c**) of semi-thin cross-sections (transversal), on BSE-SEM images (**d**) of polished slices (uranyl acetate-stained) and on SE-SEM images of freeze-fractured aegagropiles (**e–g**) or isolated fibres (**h**) of **a** Thin fibre identified as by fibre bundle from stems (rhizomes) showing a degraded zone (1), **b** Flat fibre identified as a sub-epidermal fibre bundle or sclerenchyma from sheath or leaf (2), **c** Wide fibre identified as poorly degraded fragment of rhizome containing several tissues and mainly parenchyma cells that separate from each other as a result of the degradation process (3), **d** Centre zone of a heterogeneous aegagropile showing mineral particles (bright, 4) and sectioned fibres (in medium grey) embedded in resin (dark grey, 9). The fibres include: wide fibres (5), flat fibres in transversal section (6), flat fibres in longitudinal section (7) and thin fibres in transversal section (8). **e** Fractured wide fibre showing round-shaped fibre bundles or 2 thin fibres (10) still attached by parenchyma (11) **f** Flat fibre showing a layer of sclerenchyma cells (14) (fibre-cells) covered by the epidermis typically from *P. oceanica* sheaths (13). Note alterations of the outer epidermal cell wall (12) **g** Flat fibre of sub-epidermal sclerenchyma (monolayer of fibre-cells) **h** Isolated thin fibre showing its longitudinal separation into thinner fibres (15)



into three morphotypes, shown to come from different plant tissues (Fig. 10).

Components of aegagropiles

The observations and analytical results showed that Mediterranean aegagropiles have both organic and mineral fractions,

i.e. a meshwork of fibres from *P. oceanica* and a variety of mineral particles forming a cemented core (Fig. 10). Three different types of fibres were distinguished by width: 0.142 ± 0.051 mm for the thin fibres, 0.462 ± 0.095 mm for the flat fibres and 2.295 ± 1.380 mm for the wide fibres. SEM observations revealed the presence of microorganisms and the alterations of the lateral cell walls, leading to the

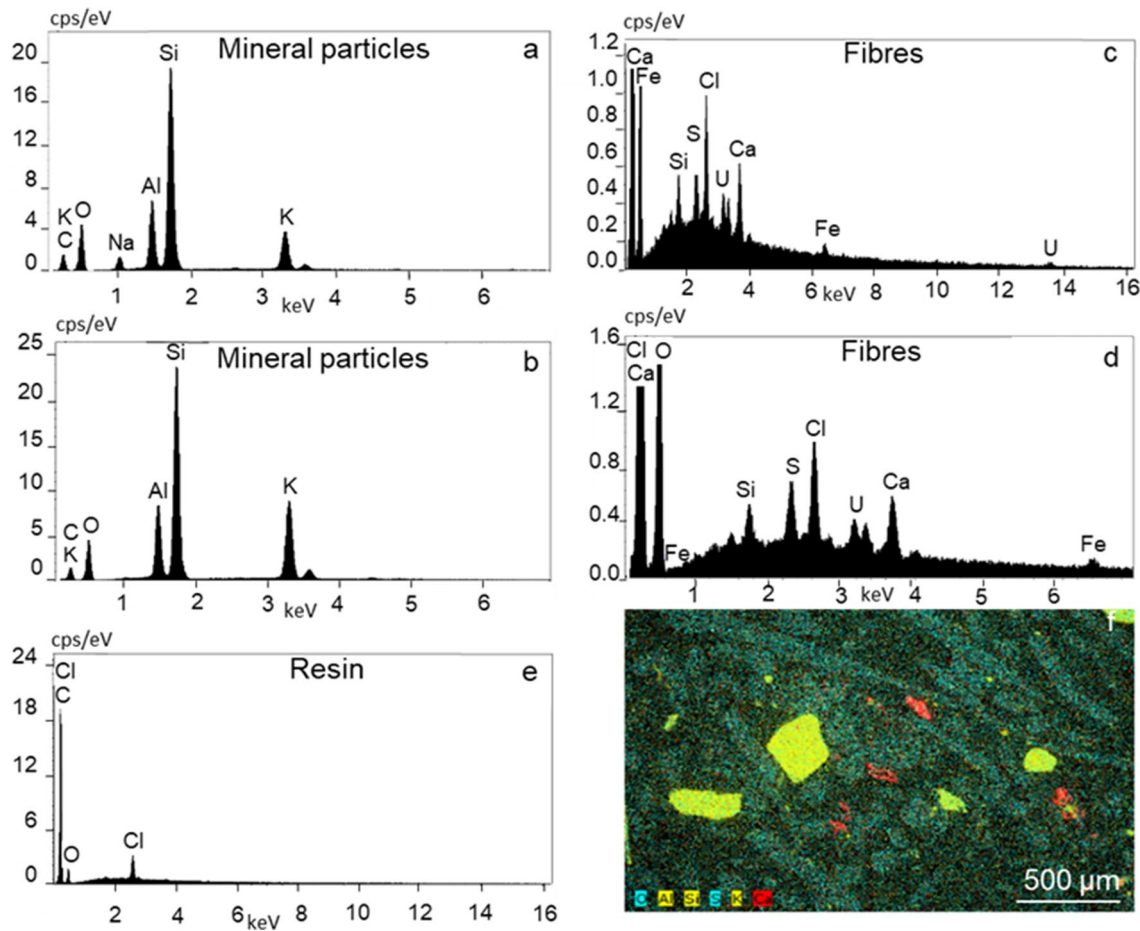


Fig. 9 Elemental X-ray spectra and mapping of different items on polished uncoated sections (uranyl acetate stained) of *P. oceanica* aegagropiles. Spectra were acquired in low-vacuum conditions with focussed position beam and maximum 50,000 counts. The X-ray energy is reported in abscissa, and the number of counts in ordinate,

a, b spectra from mineral particles **c, d** spectra from fibres, **e** spectrum performed on the resin, **f** elemental X-ray mapping performed in the central zone of an aegagropile (Fig. 9d) by use of K α peaks of the elements: O and S in blue. Al, Si and K in yellow. Ca in red

formation of fibres by longitudinal separation of cells along the middle lamella. Differences between fibre types and widths can be explained by their histological origin and their degradation from microorganism activity (e.g. bacteria and fungi) and hydrodynamics (Lemke et al. 2007; Nilsson and Singh 2014; Vohnik et al. 2015, 2016, 2019). The primary plant debris found in aegagropiles was superficial fragments of leaves and leaf sheaths, including sub-epidermal sclerenchyma with or without epidermis in the case of flat fibres as well as isolated fibre bundles (of sclerenchyma cells) from and rhizomes for the thin and wide fibres, all from *Posidonia oceanica*. The wide fibres were mainly fragments of poorly degraded rhizomes that include several tissues, while the thin fibres appeared to be the end product of degradation, consisting only of highly lignified fibre bundles of many or few cells, like those shown by various authors (Gunning and Pate 1969; Gunning 1977; Larkum 1989; Olesen et al. 2002; Larkum et al. 2007; Nilsson and Singh 2014). This

outcome was expected since the litter of the *P. oceanica* meadow is mainly composed of leaves falling throughout the year, as well as pieces of rhizomes (Crouzet 1981; Boudouresque et al. 2006; Simeone and De Falco 2012). Research has proved that the majority of the fibres composing these aegagropiles comes from the leaf sheaths and rhizomes of the plant (De los Santos et al. 2016). Approximately 25 *P. oceanica* shoots comprised one aegagropile.

The aegagropile formations found on the Mediterranean beaches (Calvi, Corsica) analysed during this study were monospecific plant agglomerations, where only the seagrass fibres were preserved (Verhille and Le Gal 2012, 2013). The lack of other photosynthetic organisms, such as algae (e.g. red, brown), can be the result of their easier (and thus earlier) degradation due to the absence of tissue organisation and of lignified cell walls. Nevertheless, we do not exclude the fact that terrigenous elements (plastics, textile fibres, elements of terrestrial plants, etc.) may be found within the

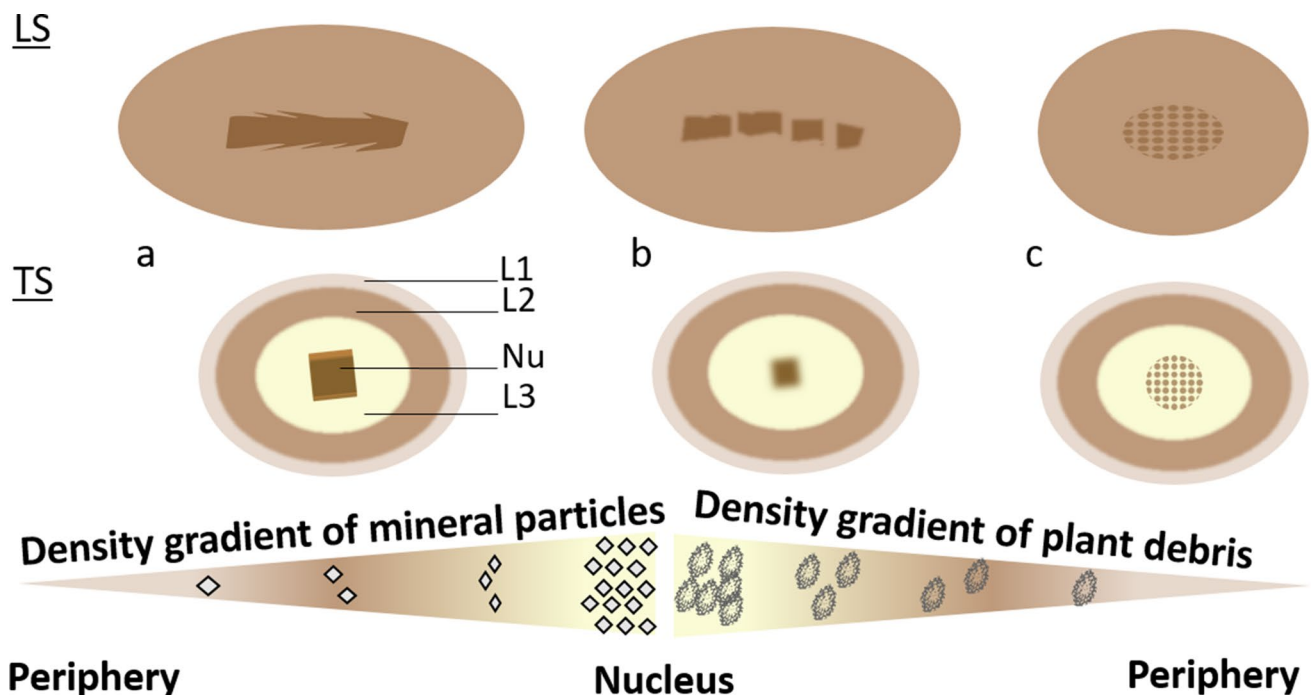


Fig. 10 Diagram illustrating the distribution of mineral particles and plant debris through a transversal cross-section of *Posidonia oceanica* aegagropiles, **a** aegagropile with a dark nucleus representing a piece of rhizome with little or no degradation (heterogeneous aegagropiles), **b** aegagropile having an intermediate morphotype with a degrading nucleus and **c** aegagropile having a denser nucleus where degradation is complete (homogeneous aegagropiles). The two triangle-shaped

diagrams illustrate the density of mineral particles (left with diamond symbols) and plant debris (right with cross-section symbols) within aegagropiles as they move from the periphery to the centre (nucleus) of the structure. L1. Layer 1, L2. Layer 2, L3. Layer 3 (=Cement), Nu. Nucleus. Symbols: dark brown square: rhizome, dark brown square with cloudy edges: rhizome in degradation, circle with brown point: last level of degradation (the rhizome bundles)

composition of aegagropiles, but none of them was found in the present study.

Mineral particles belong mainly to silicates and carbonates, as shown in X-ray elemental spectra and mappings. Silicate particles are rich in Si, O and Al and can contain K and/or Na. They likely correspond to alumino-silicate particles that could include feldspar or micas and probably come from the sediment. Carbonate particles always contain Ca, thus having a Ca-carbonate composition. These particles are interpreted as fragments of calcified remains from marine organisms; their shape, sometimes recognisable, supports this biological origin. Both silicate and carbonate particles are undoubtedly particles of sediment that accumulate inside aegagropiles during their formation, i.e. rolling on sandy areas of the sea floor.

Types and internal architecture of aegagropiles

The collected Mediterranean aegagropiles were either ellipsoidal (egg-shaped; 79%) or spheroidal in shape (ball-shaped; 21%). The ellipsoidal shape correlated in almost 60% of the cases with the heterogeneous type of aegagropiles, i.e. possessing a rhizomic nucleus, while all of the spheroidal aegagropiles were of the homogeneous or

intermediate type. Both shapes of aggregations have also been observed in algae and plant balls such as those from *Cladophora* sp. Kütz (1843), *Enteromorpha* sp. Link (1820), *Ulva* sp. Linnaeus (1753) for Chlorophyta species, *Dictyota* sp. J.V. Lamour (1809) for Phaeophyta species and *Spartina* (Schreb., 1789) (Mathieson et al. 2015) for Plantae species. The spheroidal shape probably results from frequent changes in directions of movements during formation (Vadas and Beal 1987; Ballantine et al. 1994). The *P. oceanica* aegagropiles consist of clustered fibres and mineral particles, giving a high mean density of 0.223 ± 0.04 g/cm³ (Oltmanns 1906; Mathieson et al. 2015). Furthermore, this density value does not allow the aegagropiles to float (more than the time that the water is inserted into the entire structure), which contrasts with the seaballs formed by *Cladophora* sp (Chlorophyta) and *Ruppia maritima* Linnaeus (1753) (Angiosperm, Monocotyledonae, Alismatales) (Acton 1916; McAtee 1925; Kindle 1934).

The internal architecture of aegagropiles with four concentric layers could be described in terms of 2 extreme types of aegagropiles with a range of intermediates. The first type was heterogeneous, in which the nucleus was a nearly intact piece of rhizome (stem of *P. oceanica*). In comparison, the second type was homogeneous, with a dense fibrous nucleus

consisting mainly of rhizome fibre bundles (thin fibres). We hypothesise that homogeneous aegagropiles are the final breakdown result of the heterogeneous type. Indeed, the nuclei of both types of aegagropiles seemed to originate from the same plant organ, the rhizome, but with different degrees of breakdown. The intermediate types of aegagropiles also showed either several short rhizome fragments or a proportion of wide fibres (not fully broken down) in their nucleus. The heterogeneous aegagropiles, those with a visible woody nucleus, could therefore be considered younger than homogeneous aegagropiles. In the latter, the nucleus was formed by densely packed fibres from vascular bundles as the latest remnants of stem degradation. Because they almost exclusively consisted of sclerenchyma cells and xylem cells, with lignin-rich cell walls, they were obviously the most resistant plant tissue and the last to undergo microbial as well as mechanical alteration (Schwarze 2007).

Similar layered architecture exists in other ball-shaped agglomerations of plant debris, but they exhibit only 3 layers instead of 4. This is the case for *Grimmia ovalis* (Hedw.) Lindb (1904)/Bryophyta balls and *Cladophora* sp. Chlorophyta balls (Acton 1916; Kindle 1934; Beck et al. 1986), which have a harder outer shell that is different from the rest of the structure. As with the peripheral layer of *P. oceanica* aegagropiles, this shell is composed of thin undercrossing filaments but is barely 5 mm thick. The central cavity of the balls formed by *G. ovalis* is brown, due to dead plant debris and a high concentration of minerals collected during its formation (Beck et al. 1986). Balls formed by *Cladophora* sp. also have a central cavity full of water, gas and minerals (Acton 1916; Kindle 1934).

Posidonia oceanica aegagropiles contrast with other fibrous seaballs in that they are made from lignin-rich thin fibres, i.e. degradation-resistant inner tissues from vascular plant organs. These fibres appear to be the final result of deep mechanical and microbiological alteration. The fact that long thin fibres or fibre bundles are predominant in the outer layer, while flat fibres or sub-epidermal sclerenchyma with or without epidermis are more common in the internal layers (always between 20 and 30% in the layers 2, 3 and nucleus), also suggests that the type of fibres could be important in ball formation. The long thin fibres may form a highly interwoven and protective outer layer as appears to be the case in other seaballs (*Grimmia ovalis* and *Cladophora* sp.) having a dense outer wall and a hollowed centre. Differing again from the other seaballs, *P. oceanica* aegagropiles are characterised by a rhizomic or a dense fibrous nucleus. Moreover, the inner layer (L 3) and the nucleus (Nu) are rich in wide fibres in heterogeneous aegagropiles ($44 \pm 9\%$ and $19 \pm 6\%$, respectively). In contrast, thin fibres dominate in the homogeneous type ($76 \pm 2\%$ and $47 \pm 14\%$), in which the proportion of wide fibres is drastically reduced ($5 \pm 3\%$ and $28 \pm 16\%$). This finding suggests that the progressive

degradation of the woody rhizomic nucleus progressively transforms the innermost wide fibres into thinner ones. When the rhizomic nucleus disappears, it only leaves a few wide fibres and many thin fibres and isolated vascular bundles.

Therefore, we propose that the layered architecture of *P. oceanica* aegagropiles is the consequence of 2 processes taking place simultaneously: the accumulation of debris around a nucleus and a continuous breakdown of the constituents of the nucleus and the outer layers. In addition, a loss of short fibres (thin fibres), which would occur at an advanced stage of degradation, would also leave only the long and thin fibres (bundles) on the surface of the aegagropiles.

Inferred formation and evolution of aegagropiles

The *Posidonia oceanica* meadow produces a large amount of plant debris from different plant organs (leaves, leaf sheaths, rhizomes and roots) at different rates to annually fuel the *P. oceanica* litter. These plant parts undergo the effects of hydrodynamics on the sea floor (ripple marks) as well as at the tidal zone where the waves lick the beach. The alteration of *Posidonia oceanica* debris is a long process involving a sequence of steps. It begins with the leaching of cytoplasmic and soap components, followed by sequential degradation of the plant cell walls by the alternating action of various bacterial and fungal microorganisms under anoxic and oxic phases, fungi and tunnelling bacteria being the only microorganisms able to degrade lignin-rich cell wall layers in the presence of oxygen (Lemke et al. 2007; Nilsson and Singh 2014; Vohnik et al. 2015, 2016, 2019; Remy et al. 2018). The sequence also involves the mechanical action of water movement as well as of specific species of the macro-fauna, namely amphipods occurring at different steps of degradation (Verhille and Le Gal 2012, 2013; Remy et al. 2018; Trevisan 2018).

Additionally, these more or less spherical agglomerates form within small depressions where swirls are engulfed. This description is similar to that of ripple marks forming on the seabed (Cannon 1979). The back-and-forth movements combined with swirls in the ripple marks result in the agglomeration of different plant debris (Ganong 1905; Mackay 1906; Mathieson and Dawes 2002; Olson et al. 2005; Verhille and Le Gal 2012, 2013; Mathieson et al. 2015). The PCA showed a higher preferential presence of long sections in the outer layers of the aegagropiles cut longitudinally and a higher number of transverse fibres in aegagropiles cut transversely. It can be confirmed from these two assumptions that aegagropiles are formed by rolling in a single direction in the ripple marks, which would explain the greater proportion of heterogeneous ellipsoid aegagropiles compared to spheroidal homogeneous ones. This finding contradicts the hypotheses of formation envisaged for the algae balls of

Cladophora sp. and *Ruppia maritima*, where the hypothesis for advanced formation involved a soft substrate at a shallow depth (McAtee 1925; Ballantine et al. 1994).

Thanks to all of our results we imagined the different steps that could lead to the formation of *P. oceanica* aegagropiles, however these different steps are only hypotheses and were not observed in situ (Supplement data 1). The “life” of *Posidonia oceanica* aegagropiles could thus be described in three phases: (1) an initiation phase around a rhizomic nucleus, (2) a growth and division phase by accumulation/separation cycles and, finally, (3) a breakdown and rounding phase until sedimentation or complete mechanical destruction is reached. The starting point would be the formation of the litter. The plant debris that makes up the litter would then be transported to areas of ripple marks where unidirectional formation would take place as supported by the PCA. Initially, a fragment of rhizome (identified by microscopic observation) would become entangled in other debris that inserts between the rhizome and the basal sheath remains that the rhizome piece bears laterally. This step would form the rhizomic core, i.e. the nucleus of heterogeneous aegagropiles observed by the μ CT scan. The nucleus would then be consolidated by added mineral particles (identified by elemental mapping) from the sediment that stabilise the central core, acting as cement (Fig. 10). The mineral particles interspersing the fibres may limit their movements, notably gliding, thus maintaining a dense interlace. When the core is formed, Layer 3, composed of a significant portion of minerals forming a compact and white cement around the nucleus visible at the naked eye, will reinforce the core (Fig. 10). Such high concentration of mineral particles in the seaball centres has already been observed in alpine moss balls *Grimmia ovalis* and algae *Gelidiopsis variabilis* (Greville ex J. Agardh) rhodophyta (Acton 1916; Kindle 1934; Beck et al. 1986). From this point on, the newly formed aegagropile has reached the critical size and is stable enough to incorporate other *P. oceanica* debris, notably fibres forming the L 2 and L 1. Over time and via hydrodynamics, the latter may undergo random fragmentation when critical length is reached. This splitting process might generate new aegagropiles of shorter length, and the growth process may continue. Subjected to hydrodynamics and the degradation of the nucleus, these aegagropiles will round off and become similar to the spheroidal (ball-shaped) aegagropiles (Cannon 1979; Verhille and Le Gal 2012, 2013). During these successive formation steps, the plant debris, and notably the nucleus, unarguably continue to undergo mechanical erosion and microbial degradation. This degradation starts during the second phase, while larger aegagropiles are being split and then rounded. Wide fibres delaminate into thinner ones and break into small segments that are likely lost from outer layers. In parallel, the nucleus is fragmented by the degradation of parenchyma between hard tissues, namely

sub-epidermal sclerenchyma of leaf sheaths and fibre bundles of rhizomes (Fig. 10). This process can gradually generate new fibres that will insert themselves into the internal layers of aegagropiles. However, the loss of a long, rigid, rhizomic nucleus helps the aegagropiles to roll in different directions. While the rounding could occur by incorporation of new fibres, it seems rather likely to result from erosion of the elongated ends of the ellipsoidal-shaped aegagropiles with a degrading nucleus. When the nucleus has disappeared, the aegagropiles are spheroidal or ball-shaped. This outcome is supported by the fact that ball-shaped aegagropiles are always homogeneous, lacking of a rhizomic nucleus and characterised by a lower diameter than the heterogeneous ones. This phenomenon supposes that the degradation of the nucleus precedes the rounding and is supported by the observations of heterogeneous aegagropiles with a fragmented nucleus.

However, the present study did not yield any direct information about the timeframe of aegagropile formation, growth and breakdown underwater or on beaches. Thus, the age of aegagropiles found on beaches remains questionable. Nevertheless, agreeing with the formation and evolution processes inferred from the results implies a yearly seasonal timescale that could determine the aegagropile lifetime. Indeed, it is known that the litter is seasonally fuelled in autumn from the meadows and degrades within six to nine months, mainly in spring and summer (Romero et al. 1992; Remy et al. 2018). The degradation of the litter undoubtedly produces fibres that may seasonally fuel the formation of aegagropiles. The time they spend in growth in ripple marks remains unknown but logically depends on seasonality. The aegagropiles could then be exported to beaches, perhaps with less regularity, during autumnal or winter storms, thus starting their aerial breakdown. This supposition allows us to place the aegagropiles in the same timeframe as the life cycle of *P. oceanica*. A regular seasonal beaching of aegagropiles (with peaks of stranding during storms) is likely followed by rapid aerial breakdown over a few months as supported by the lack of evidence of long-term terrestrial accumulation of aegagropiles (i.e. over years). However, as aegagropiles found on beaches seem to be at different stages of their lifecycle, it can be supposed they are of different ages. Possibly, the more degraded ones have remained two—or several—years underwater. That said, the different steps might also reflect that the formation of aegagropiles starts at different times over a rather long period (6–9 months) of fibre production by leaf export from meadow and litter degradation. Thus, because their formation and breakdown depend on seasonal events, there is no real reason to consider that the lifetime of aegagropiles surpasses one lifecycle of *P. oceanica*. Nonetheless, the possibility that aegagropiles have a regular or exceptional lifetime over two or several years cannot be excluded. Furthermore, aegagropiles, by their

formation, decrease the quantity of litter from *Posidonia* that accumulates on the seabed (ripple marks, abyss). Some will be exported to the abyss and others to the beaches. The aegagropiles washed up on the beaches are not included in the banquettes of *P. oceanica*. Accordingly, the carbon cycle within the *P. oceanica* ecosystem should be re-evaluated to include aegagropiles (terrestrial and submarine).

Conclusion

Very little was previously known about the aggregations of *Posidonia oceanica* fibrous debris named “aegagropiles”. Using several methods of observation and characterisation at different scales, this study described their shape, density, composition, formation and internal structure. These high-density aegagropiles (0.21 g/cm^3), collected along the beaches of the Mediterranean Sea, are mainly ellipsoidal and are composed of several concentric layers that are distinguishable by their plant fibres and mineral particle concentrations as well as by their fibre types, orientation and degradation.

All these observations allowed us to propose a possible formation/breakdown scenario for these aegagropiles: starting from plant debris carried out of the meadow and litter to aggregation in ripple marks around a rhizomic nucleus and separation from an original elongated structure, ending as complex fibrous balls on the beaches where mechanical breakdown by wind can occur. The results provide neither a direct estimation of the time required for formation of the aegagropiles nor their age. However, the *P. oceanica* ecosystem is regulated seasonally and annually. This understanding could therefore allow us to assume that the entire process of formation and degradation could very well take place within the time frame of a few months to several years. The beaching of aegagropiles at different formation stages and lack of evidence of long-term terrestrial accumulation of aegagropiles suggest their rapid aerial breakdown rather than a hypothetical return to the sea.

Finally, estimating that one aegagropile (density of 0.2 g/cm^3) represents approximately 25 *Posidonia* shoots (De los Santos et al. 2016), while the number of aegagropiles per beach surface is currently unknown, in view of the number of aegagropiles observable each year on Mediterranean beaches, it can be concluded that their importance is not negligible in the carbon cycle. As they were neglected to date in the models, the amount of carbon represented by the *Posidonia oceanica* meadows is probably undervalued because aegagropiles constitute a pool of carbon on beaches, such as in the “banquettes” and the litter.

Supplementary Information The online version contains supplementary material available at <https://doi.org/10.1007/s00227-021-03833-y>.

Acknowledgements This work is part of the STARE-CAPMED project funded by the STARESO Institute, the Territorial Collective of Corsica (CTC) and the Rhône Mediterranean Corsica Water Agency. The authors also thank Mrs Sarah Smeets for her excellent technical assistance. The authors thank the Center for Applied Research and Education in Microscopy (CAREM-Ulège) for providing access to electron microscopy equipment. This work was also supported by the Fonds National de la Recherche Scientifique (FNRS, Belgium). E.P. (post-doctoral researcher) has a mandate supported by the FNRS. The MARE publication number for this document is MARE401.

Author contributions All authors contributed to the study conception and design. Material preparation, data collection and analysis were performed by LL, EP, AL, PC and SG. The first draft of the manuscript was written by LL and all authors commented on previous versions of the manuscript. All authors read and approved the final manuscript.

Funding This work is part of the STARE-CAPMED project funded by the STARESO Institute, the Territorial Collective of Corsica (CTC) and the Rhône Mediterranean Corsica Water Agency and also supported by the Fonds National de la Recherche Scientifique (FNRS, Belgium). E.P. (post-doctoral researcher) has a mandate supported by the FNRS.

Compliance with ethical standards

Conflict of interest The authors do not have any conflict of interest.

Consent for publication Yes, all of the authors consent for the publication.

Data availability statement The datasets generated during and/or analysed during the current study are available from the corresponding author on reasonable request.

References

- Abadie A, Lejeune P, Pergent G, Gobert S (2016) From mechanical to chemical impact of anchoring in seagrasses: the premises of anthropogenic patch generation in *Posidonia oceanica* meadows. *Mar Pollut Bull* 109(1):61–71
- Acton E (1916) On the structure and origin of “*Cladophora* Balls”. *N Phytol* 15:1–5
- Austin AP (1960) Observations on *Furcellaria fastigiata* (L.) Lam. forma aegagropila Reinke in Danish waters together with a note on other unattached algal forms. *Hydrobiol Int J Aquat Sci* 14:255–277
- Ballantine DL, Aponte NE, Holmquist JG (1994) Multi-species algal balls and potentially imprisoned fauna: an unusual benthic assemblage. *Aquat Bot* 48:167–174
- Beck E, Mägdefrau E, Senser M (1986) Globular mosses. *Flora* 178:73–83
- Boudouresque CF, Meinesz A (1982) Découverte de l’herbier de Posidonies. *Cahiers du Parc National de Port Cros* 4:1–79
- Boudouresque CF, Bernard G, Bonhomme P, Charbonnel E, Diviacco G, Meinesz A, Pergent G, Pergent-Martini C, Ruitton S, Tunesi L (2006) Préservation et conservation des herbiers à *Posidonia oceanica*. Ramoge. ed
- Cannon JFM (1979) An experimental investigation of *Posidonia* balls. *Aquat Bot* 6:407–410

- Coletti A, Valerio A, Vismara E (2013) *Posidonia oceanica* as a renewable lignocellulosic biomass for the synthesis of cellulose acetate and glycidyl methacrylate grafted cellulose. *Materials* 6(5):2043–2058
- Crouzet A (1981) Mise en évidence de variations cycliques dans les écailles des rhizomes de *Posidonia oceanica* (Potamogetonaceae). *Trav. Sci. Parc Nation, Port-Cros*
- De los Santos CB, Vicencio-Rammsy B, Lepoint G, Remy F, Bouma TJ, Gobert S (2016) Ontogenic variation and effect of collection procedure on leaf biomechanical properties of Mediterranean seagrass *Posidonia oceanica* (L.) Delile. *Mar Ecol* 37(4):750–759
- Duarte CM, Cebrián J (1996) The fate of marine autotrophic production. *Limnol Oceanogr* 41
- Duarte CM, Chiscano CL (1999) Seagrass biomass and production: a reassessment. *Aquat Bot* 65:159–174
- Duarte CM, Middelburg J, Caraco N (2005) Major role of marine vegetation on the oceanic carbon cycle. *Biogeosciences* 1:659–679
- Ganong WF (1905) On balls of vegetable matter from Sandy Shores. *Rhodora* 7:41–47
- Giraud G (1977) Recensement des floraisons de *Posidonia oceanica* (Linné) Delile en Méditerranée. Marseille cedex 2
- Gobert S, Kyramarios M, Lepoint G, Pergent-Martini C, Bouqueneau J (2002) Variations à différentes échelles spatiales de l'herbier à *Posidonia oceanica* (L.) Delile ; effets sur les paramètres physico-chimiques du sédiment. *Oceanol Acta* 26:199–207
- Gobert S, Cambridge ML, Velimirov B, Pergent G, Lepoint G, Bouqueneau J-M, Dauby P, Pergent-Martini C, Walker DI (2006) Biology of *Posidonia*. In: Larkum AWD, Orth RJ, Duarte CM (éds) *Seagrasses: biology, ecology and conservation*. Springer, pp 387–408
- Gunning BES (1977) Transfer cells and their roles in transport of solutes in plants. *SciProg* 64:539–568
- Gunning BES, Pate JS (1969) “Transfer cells” plant cells with wall ingrowths, specialized in relation to short distance transport of solutes—their occurrence, structure, and development. *Protoplasma* 68:107–133
- Hayat M (1993) Stains and cytochemical methods, plenum pre. Plenum Publishing Corporation, New York and London
- Hemminga MA, Duarte CM (2000) *Seagrass ecology*. The Press syndicate of the university of Cambridge, Cambridge Kingdom
- Holdsworth DW, Thornton MM (2002) Micro-CT in small animal and specimen imaging. *Trends Biotechnol* 20:34–39
- Hosogi N, Nishioka H, Nakakoshi M (2015) Evaluation of lanthanide salts as alternative stains to uranyl acetate. *Microscopy* 64:429–435
- Kindle EM (1934) Lake balls, “*Cladophora* balls” and coal balls. *Am Midl Nat* 15:752–760
- Kuo J, den Hartog C (2007) Seagrass morphology, anatomy, and ultrastructure. In: Larkum AWD, Orth RJ, Duarte CM (éd) *Seagrasses: biology, ecology and conservation*. Springer, pp 51–87
- Kuo J, Stewart JG (1995) Leaf anatomy and ultrastructure of the North American marine angiosperm *Phyllospadix* (Zosteraceae). *Can J Bot* 73:827–842
- Laffoley D, Grimsditch G (2009) The management of natural coastal carbon sinks. IUCN, Gland
- Larkum AW (1989) *Biology of seagrass: a treatise on the biology of seagrasses with special reference to the Australian region*. Elsevier Science Limited, Californie
- Larkum AWD, Orth RJ, Duarte CM (2007) *Seagrasses: biology, ecology and conservation*. Springer, Dordrecht
- Lemke AM, Lemke MJ, Benke AC (2007) Importance of detrital algae, bacteria, and organic matter to littoral microcrustacean growth and reproduction. *Limnol Oceanogr* 52:2164–2176
- Lepot K, Compère P, Gérard E, Namsaraev Z, Verleyen E, Tavernier I, Hodgson DA, Vyverman W, Gilbert B, Wilmotte A, Javaux EJ (2014) Organic and mineral imprints in fossil photosynthetic mats of an East Antarctic lake. *Geobiology* 12:424–450
- Mackay AH (1906) Water-rolled Weed-balls. *Proc Nov ScotianInstSci* 11:1902–1906
- Mathieson AC, Dawes CJ (2002) *Chaetomorpha* balls foul New Hampshire, USA Beaches. *Algae* 17:283–292
- Mathieson AC, Dawes CJ, Lull WW (2015) Mystery beach balls foul long island, NY, beaches. *Rhodora* 117:92–97
- Mathieson AC, Hehre EJ, Dawes CJ (2016) Aegagropilous *Desmarestia aculeata* from New Hampshire. *Rhodora* 102:202–207
- McAtee WL (1925) Notes on drift, vegetable balls, and aquatic insects as a food product of inland waters. *Ecology* 6:288–302
- Nilsson T, Singh AP (2014) Tunnelling bacteria and tunnelling of wood cell walls, vol 1. McGraw-Hill, New York, pp 395–399
- Olesen B, Enriquez S, Duarte CM, Sand-Jensen K (2002) Depth-acclimation of photosynthesis, morphology and demography of *Posidonia oceanica* and *Cymodocea nodosa* in the Spanish Mediterranean Sea. *Mar EcolProgSer* 236:89–97
- Olson RW, Schmutz JK, Hammer UT (2005) Occurrence, Composition and Formation of *Ruppia*, Widgeon grass, balls in Saskatchewan Lakes. *Can Fied Nat* 119:115–119
- Oltmanns F (1906) *Morphologie und Biologie der Algen*
- Pergent G (1990) Lepidochronological analysis of the seagrass *Posidonia oceanica* (L.) Delile: a standardized approach. *Aquat Bot* 37:39–54
- Pergent G, Romero J, Pergent-Martini C, Mateo MA, Boudouresque CF (1994) Primary production, stocks and fluxes in the Mediterranean seagrass *Posidonia oceanica*. *Mar EcolProgSer* 106:139–146
- Remy F, Mascart T, De troch M, Michel LN, Lepoint G (2018) Seagrass organic matter transfer in *Posidonia oceanica* macrophyto-detritus accumulations. *Estuar Coast Shelf Sci* 212:73–79
- Romero J, Pergent G, Pergent-Martini C, Mateo M-A, Regnier C (1992) The Detritic compartment in a *Posidonia oceanica* meadow: litter features, decomposition rates, and mineral stocks. *Mar Ecol* 13:69–83
- Schwarze FWMR (2007) Wood decay under the microscope. *Fungal Biol Rev* 21:133–170
- Simeone S, De Falco G (2012) Morphology and composition of beach-cast *Posidonia oceanica* litter on beaches with different exposures. *Geomorphology* 151:224–233
- Smith NM, Walker DI (2002) Canopy structure and pollination biology of the seagrasses *Posidonia australis* and *P. sinuosa* (Posidoneaceae). *Aquat Bot* 74:57–70
- Trevisan M (2018) Recherche et caractérisation de symbioses microbiennes chimiosynthétiques ou digestives chez des crustacés amphipodes associés à des accumulations végétales en milieux marins côtier et profonds. Université de Liège, Thesis, p 307
- Vacchi M, Montefalcone M, Bianchi CN, Morri C, Ferrari M (2012) Hydrodynamic constraints to the seaward development of *Posidonia oceanica* meadows. *Estuar Coast Shelf Sci* 97:58–65
- Vadas RL, Beal B (1987) Green algal ropes: a novel estuarine phenomenon in the Gulf of Maine. *Estuaries* 10:171–176
- Verhille G, Le Gal P (2012) Formation des aegagropiles: compaction d’une pelote de poils par un écoulement. In: 15e Rencontre du Non-Linéaire Paris 2012, vol 12, p 1
- Verhille G, Le Gal P (2013) Sur la compaction de fibres et la formation des aegagropiles. In: 21e Congrès Français de Mécanique, Bordeaux, pp 1–6
- Vizzini S, Sarà G, Mateob MA, Mazzola A (2003) $\delta^{13}C$ and $\delta^{15}N$ variability in *Posidonia oceanica* associated with seasonality and plant fraction. *Aquat Bot* 76:195–202
- Vohnik M, Borovec O, Zupan I, Vondrasek D, Petrtl M, Sudova R (2015) Anatomically and morphologically unique dark septate endophytic association in the roots of the Mediterranean endemic seagrass *Posidonia oceanica*. *Mycorrhiza* 25:663–672

- Vohník M, Borovec O, Kolařík M (2016) Communities of cultivable root mycobionts of the seagrass *Posidonia oceanica* in the Northwest Mediterranean Sea are dominated by a hitherto undescribed pleosporalean dark septate endophyte. *Microb Ecol* 71:442–451
- Vohník M, Borovec O, Kolaříková Z, Sudová R, Réblová M (2019) Extensive sampling and highthroughput sequencing reveal *Posidoniomyces atricolor* gen. et sp. nov. (Aigialaceae, Pleosporales) as the dominant root mycobiont of the dominant Mediterranean seagrass *Posidonia oceanica*. *MycKeys* 55:59–86
- Wilce RT, Schneider CW, Quinlan AV, Bosch KV (1982) The life history and morphology of free-living *Pilayella littoralis* (L.) Kjellm. (Ectocarpaceae, Ectocarpales) in Nahant Bay, Massachusetts. *Phycologia* 21:36–354

Publisher's Note Springer Nature remains neutral with regard to jurisdictional claims in published maps and institutional affiliations.